Controlled Diels−Alder Reactions Used To Incorporate Highly Efficient Polyenic Chromophores into Maleimide-Containing Side-Chain Polymers for Electro-Optics

Zhengwei Shi,[†] Jingdong Luo,[†] Su Huang,[†] Yen-Ju Cheng,[†] Tae-Dong Kim,[†] Brent M. Polishak,[‡] Xing-Hua Zhou,[†] Yanqing Tian,[†] Sei-Hum Jang,[†] Daniel B. Knorr, Jr.,[§] René M. Overney,[§] Todd R. Younkin,[||] and Alex K.-Y. Jen*[,†,‡]

Department of Materials Science and Engineering, Department of Chemistry, and Department of Chemical Engineering, University of Washington, Seattle, Washington 98195, and Components Research, Intel Corporation, Hillsboro, Oregon 97124

Received November 20, 2008; Revised Manuscript Received February 6, 2009

ABSTRACT: Using an *in situ* Diels−Alder (DA) "click chemistry" strategy for reactions between anthracene and maleimide functional groups, two prototypes of novel nonlinear optical (NLO) side-chain polymers (**PMI-A7** and **PMI-B7**) containing highly hyperpolarizable but chemically sensitive phenyltetraene-based chromophores were synthesized and their nonlinear optical and thermal properties were characterized. Through rational material design, these NLO side-chain polymers exhibited good processibility, large electro-optic (E-O) coefficients (r_{33}, of up to 263 and 287 pm/V at 1.31 μm wavelength respectively), and excellent temporal stability. These combined properties make them promising materials for E-O device applications. Compared to **PMI-B7**, **PMI-A7** exhibited significantly enhanced temporal stability (87% of the initial r_{33} values was retained after 550 h at 85 °C) and solvent resistance, which was attributed to slight cross-linking from the side reaction between maleimide and phenyltetraenic chromophore moieties. This study showed that it is possible to take advantage of some side reactions to enhance the performance of NLO materials.

Introduction

Organic second-order nonlinear optical (NLO) materials have drawn considerable interest because of their potential applications in telecommunications and high-speed signal processing.[1,2] For device applications, NLO polymers should possess large electro-optic (E-O) activity, low optical loss, good temporal stability and processibility.[3] Macroscopic second-order NLO properties originate from the noncentrosymmetric alignment of highly polarizable NLO chromophores, either doped in a guest/host system or covalently bonded as side-chains of a polymer. When efficient NLO chromophores are doped into high T_g polymer matrices, they tend to pack and form aggregates due to strong intermolecular electrostatic interactions caused by the large dipole moment of the NLO chromophores. The difficulty of overcoming or preventing such interactions leads to low poling efficiency, fast relaxation of the polar order, and phase separation over time.[3,4] To overcome these deficiencies, side-chain polymers have been developed to prevent chromophore from separating from the polymer matrices. They also allow high chromophore loading, good homogeneity, and temporal stability.[5] A broad variety of side-chain NLO polymers have been demonstrated through postfunctionalization of commercially available polymers using the Mitsunobu reaction,[6] azo coupling,[7] tricyanovinylation,[8] Kneovenagel condensation,[9] and acid and base catalyzed esterification.[10] More recently, the "click-chemistry", based on Huisgen's 1,3-dipolar cycloadditions of azide-alkyne or Diels−Alder reactions,[11−15] has emerged as a powerful strategy to construct NLO polymers.[16,17]

Synthetic advantages of this approach include excellent conversion efficiency, mild reaction conditions, and compatibility with the poling process. Owing to better compatibility with highly polarizable NLO chromophores with cyano groups, Diels−Alder reactions have been selected as one of the most efficient "click chemistries" to construct high-performance NLO polymers.[16] Apart from synthesizing side-chain NLO polymers from tedious synthetic steps, our group has recently designed a simple protocol to achieve high-performance NLO polymers by performing *in situ* lattice hardening during the poling process.[18] This strategy effectively removes several bottlenecks in making side-chain NLO polymers, including precisely controlling the compositions and properties of NLO materials from batch to batch and tedious polymer purification. With this new methodology, high chromophore loading (up to 39 wt %) can be successfully incorporated into polymer matrices without causing phase separation, leading to large r_{33} values (of up to 110 pm/V at 1.31 μm wavelength) as well as good temporal stability.

To further improve the E-O properties of these NLO polymers, much more efficient NLO chromophores such as phenyltetraene-based chromophores were incorporated into the polymers. Phenyltetraenic chromophores consist of conjugated (4-dialkylamino)phenyltetraene bridges and the 2-dicyanomethylen-3-cyano-4-methyl-5-phenyl-5-trifluoromethyl-2,5-dihydrofuran (CF_3−Ph−TCF) acceptor. These chromophores are known to exhibit very large molecular hyperpolarizabilities (Figure 1).[19] However, the chemical reactivity of these chromophores poses major challenges in functionalizing and incorporating them into side-chain polymers (Scheme 1). In our study, through rational molecular design, two prototypes of side-chain NLO polymers (**PMI-A7** and **PMI-B7**) (Scheme 2) were developed employing two types of highly hyperpolarizable phenyltetraenic chromophores, **AJL28** and **AJL39** (Figure 1). **AJL28** shows relatively high diene reactivity toward maleimido dienophiles. In contrast, **AJL39**, one of the typical new-generation chromophores developed in our group recently, possesses very weak dienic reactivity due to the functional modification at the **R** position (Figure 1).[20] These new NLO

* E-mail: ajen@u.washington.edu.
[†] Department of Materials Science and Engineering, University of Washington.
[‡] Department of Chemistry, University of Washington.
[§] Department of Chemical Engineering, University of Washington.
[||] Components Research, Intel Corporation.

10.1021/ma802612g CCC: $40.75
Published on Web 03/06/2009

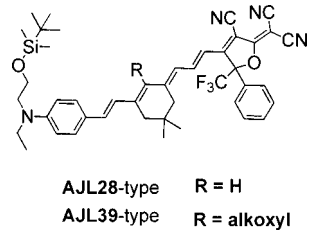

Figure 1. Selected "Push−pull" structure of phenyltetraene-based NLO chromophores with strong CF_3−Ph−TCF acceptor.

polymers are designed with several unique features. First, the NLO polymers possess higher E-O activity, because phenyltetraenic chromophores have larger hyperpolarizabilities (∼7600 × 10^{-30} esu at 1.907 μm wavelength) compared to the commonly used **FTC** chromophores (∼1180 × 10^{-30} esu at 1.907 μm wavelength).[21] Second, to effectively prevent aggregation and phase separation, we have tuned the polarity of guest−host components by implanting the highly polar maleimido dienophile moieties into the less polar polymer backbones. In addition, we have imbedded lower polarity anthryl diene groups at the peripheral site of the dipolar NLO chromophores. These substitutions result in better compatibility between chromophores and polymers, which is expected to lead to improved optical transparency. Third, in terms of processing, the polarity adjustment of the components allows a wide range of stable NLO polymers to be readily formulated by simply blending a given cross-linkable chromophore with various cross-linkable host polymers for device developments. After poling, these two NLO polymers showed large r_{33} values (of up to 263 and 287 pm/V at 1.31 μm wavelength, respectively), good temporal stability, and excellent poling characteristics. To accompany these chemical modifications, we have also conducted a systematic study for constructing high-performance NLO polymers *via* Diels−Alder-based click chemistry. This offers significant insights in developing next generation highly efficient NLO polymers.

Results and Discussion

Design, Synthesis, and Characterization. Following previous quantum mechanical calculations for chromophore design,[22] phenyltetraene-based chromophores were established as one of the most effective frameworks exhibiting very large molecular hyperpolarizabilities. There are a few reports of polyenic chromophores being successfully modified or functionalized for covalently incorporating into polymer matrices. For example, the Steglich esterification can be used with 1,3-dicyclohexylcarbodiimide (DCC) as the condensation reagent for attaching **CLD1**-type chromophores to polymer backbones,[5a] but it cannot be applied to the **AJL28**-type chromophores. The resultant reactivity is due to the stronger CF_3−Ph−TCF acceptor enhancing the ground-state charge separation along the methine skeleton of chromophores, which leads to higher chemical sensitivities even under normal reaction conditions. Thus, we prefunctionalized the anthryl group, which is designed for click chemistry, onto the donor-end of dialkylaminophenyltrienal **A5** by the DCC-mediated esterification, and the resultant bridge precursor **A6** was condensed with the CF_3−Ph−TCF acceptor at the final step to afford a new chromophore **A7** bearing the anthryl group. **B7** was prepared in good yield in a manner analogous to that for **A7** with a methoxy group imbedded in the middle of bridge to eliminate the diene-like chromophore reactivity toward maleimido dienophiles. In order to keep compounds **A7** and **B7** of similar molecular weight, a relatively short linkage was utilized in compound **B7** as compared to **A7**. The overall yield of this synthesis is above 40% after three steps, and the sequential synthesis can be used as a protocol for functionalizing these advanced polyenic chromophores.

As shown in Scheme 2, maleimide-containing copolymer (**PMI**) was prepared *via* the esterification reaction between poly(4-vinyl phenol-*co*-methyl methacrylate) (**8**) and 4-maleimido benzoyl chloride. Although the E-O activities could be improved by increasing the chromophore content in the material system, there is a threshold for the maximum amount of chromophore allowed; otherwise, it will deteriorate the poling efficiency and temporal stability of the resulting poled polymers.[18] By taking into account of this potential problem, 10 mol % of the phenolic groups on polymer **8** were converted into maleimido groups, and the remaining 40 mol % of the phenolic groups were terminated with excess acetyl chloride at the end of the reaction to obtain maleimido-containing polymer (**PMI**). If these groups could be all reacted with anthryl-containing chromophore, it should give **PMI** side-chain polymers with ∼2.55 × 10^{20} cm^{-3} chromophore content. At this number density, reasonably balanced material properties, such as good thermal stability, high poling efficiency, and optical transparency could be achieved. The FT-IR spectrum of the resultant maleimide-functionalized polymer clearly shows a lack of phenol absorbance at ∼3200 cm^{-1} compared to the original polymer **8**, which indicates the complete termination of phenolic groups. Furthermore, the presence of the maleimide peak (CH of CH═CH bond around 687 cm^{-1}) for **PMI** in the FT-IR spectrum clearly shows the successful incorporation of maleimido groups. The molar ratio of three components was confirmed by proton NMR. The integrals of protons of maleimido-phenyl moiety and methyl gorup of MMA are in the ratio of about 1 to 3.5. Gel-permeation chromatography (GPC) reveals a number-average molecular weight (M_n) of ∼12 000 for the resultant polymer. Thermal analysis by differential scanning calorimetry (DSC) shows a relatively high glass transition temperature (T_g) of 125 °C for **PMI** (ramping rate, 10 °C/min, under nitrogen).

Morphology and Near-IR Absorption Study. Generally, the polarity mismatch of two components in the guest−host material systems is often accompanied by microaggregation and phase separation, resulting in inhomogeneous broadening of chromophoric absorption.[23] However, in photorefractive (PR) and liquid-crystal (LC) systems, researchers have demonstrated that by intelligently controlling the polarity of the polymer matrices, the material can be made sufficiently resistant against phase separation and offer much better performance (a factor of 4−5) in index modulation amplitude.[24,25] In our study, by grafting highly polar maleimido dienophile moieties in pendant positions, the polarity of polymer was enhanced. The resulting copolymer **PMI** shows good compatibility with relatively high polar chromophores such as **AJL28**, **AJL39**, **A7**, and **B7**. To test the chromophoric absorptivity and stability in solid states in the presence of maleimido groups, compounds **AJL28**, **A7**, and **B7** were mixed into a solution with **PMI** (39%:61% w/w) in 1,1,2-trichloroethane. These solutions were spin-coated onto glass substrates and baked overnight at 50 °C in vacuum oven to afford thin films of **PMI/AJL28**, **PMI-A7**, and **PMI-B7** respectively. The films were optically smooth and uniform upon visual inspection by optical microscopy. Moreover, the blend morphology study by atomic force microscope (AFM) was performed to study the compatibility of **PMI-A7**. Compared to a previous morphology study of highly polar chromophore **AJT101** doped at 50 wt % in the low polarity polycarbonate matrices (Figure 2a), which showed severe microphase separation,[26] a cured film of **PMI-A7** shows no severe phase separation by AFM (Figure 2b). Thus, we can achieve excellent compatibility and homogeneous films by intelligently tuning the polarity of polymers. Furthermore, the chromophore number density

Scheme 1. Synthesis of Anthracenyl-Functionalized Phenyltetraene Chromophores A7 and B7[a]

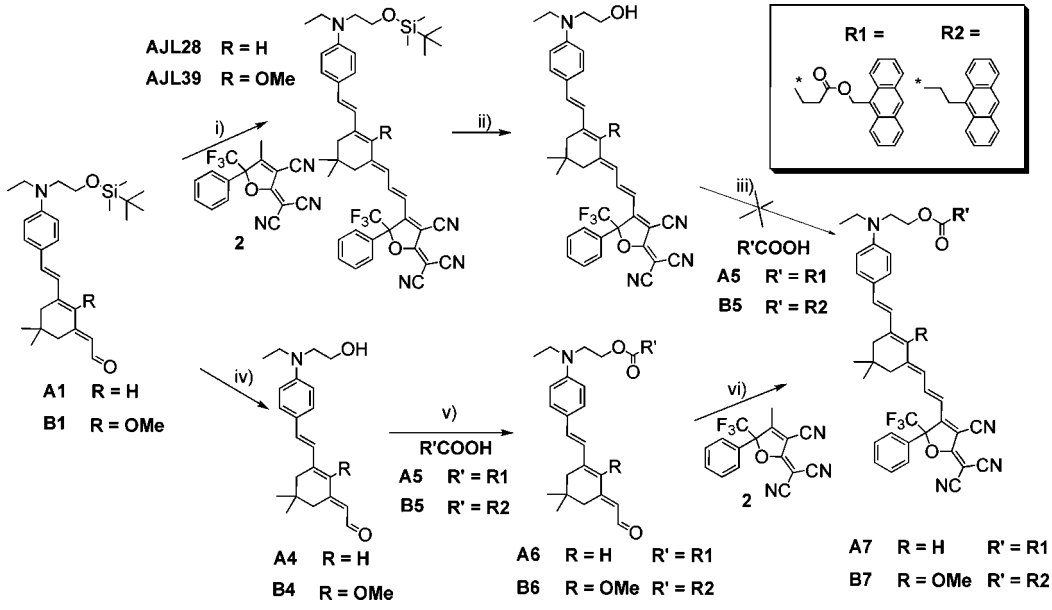

[a] Reaction conditions: (i or vi) ethanol, 60 °C; (ii or iv) 1M HCl, THF; (iii and v) 1,3-dicyclohexylcarbodiimide (DCC), (4-dimethylamino)pyridinium 4-toluenesulfonate (DPTS), CH_2Cl_2.

Scheme 2. Synthesis of a Maleimido-Containing Side Chain Polymer PMI and the Process of Diels−Alder "Click Chemistry" by Curing a Mixture of PMI and an Anthracene-Attached Chromophore A7 and B7, Respectively

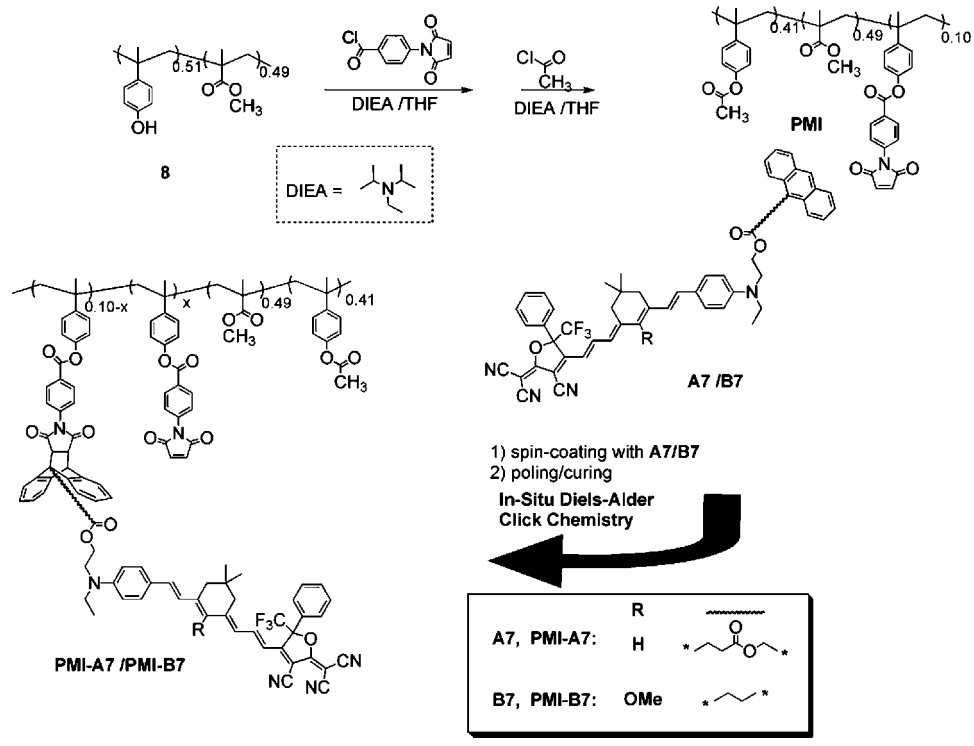

achieved is up to 2.55×10^{20} cm^{-1}, which is extremely high as compared to other guest−host NLO systems.

According to Figure 3, all the films show strong absorption bands in 600 to 1100 nm region, where the λ_{max} absorption corresponds to the intramolecular charge-transfer absorption band of the chromophores. The noncured films of **PMI-A7** show around 10 nm blue shift compared to those of **PMI/AJL28**, which is indicative of the better compatibility of **PMI-A7** than **PMI/AJL28**. This is due to the much more flexible peripheral group in compound **A7**. In addition, the UV absorption peak of **PMI/AJL28** shows more than 15 nm broadening compared to that of **PMI-A7**. This result provides another clear indication that **PMI-A7** offers much more homogeneous thin films than **PMI/AJL28**. Similarly, high quality thin films from **PMI-B7** show the wavelength of maximum absorption (λ_{max}) of the main charge-transfer band at 790 nm. This slight blue shift is ascribed to the imbedding of methoxy group in the middle of the highly polarized phenyltetraene bridge with reduced bond order alternation (BOA).[20]

After isothermal curing at 130 °C for 30 min, the absorption spectrum intensity of **PMI/AJL28** decreases by 35%. We also observed that the annealed films of **PMI/AJL28** had a slight

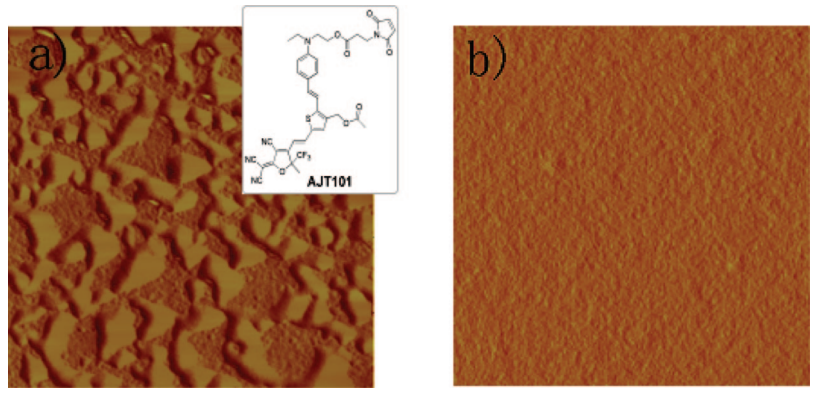

Figure 2. AFM phase images for thin films of (a) guest−host polymer **AJT101** in **APC** and (b) side-chain polymer (*in situ*) **PMI-A7**. The image size is 5 μm in both images.

increase in the secondary absorption band around the 400−500 nm regions. These major absorption changes after annealing are due to severe chromophore decomposition by maleimido dienophiles and forming less conjugated species.[27] This result is in good agreement with our previous model compound study.[20]

Under the same curing conditions, **PMI-A7** shows more stability than **PMI/AJL28**. Nearly 90% of the major chromophore absorption band is retained. This suggests that the anthracenyl group at the chromophore donor-end has a higher reactivity toward pendant maleimido moieties in polymers and can serve as a scavenger to prevent most of the doped chromophore **A7** from reacting with maleimides. Starting from a highly soluble guest−host polymer, the cured films of **PMI-A7** also have much improved mechanical properties and solvent resistance *via* the anthracene-maleimide-based DA "click chemistry". The degree of DA "click chemistry" completion was preliminarily evaluated by thin layer chromatography (TLC). The **PMI** and chromophore **A7** are easily redissolved from the noncured films, and can be separated from each other on silica gel TLC plates. After curing, the films possess significantly improved solvent resistance. Only very high polar solvents such as cyclopentanone could be used to dissolve the thin films to preliminarily monitor the reaction by thin layer chromatography (TLC). The results clearly show that ∼80% of chromophore **A7** has been incorporated into the polymer backbone, even though there is still ∼20% nonreacted chromophore **A7** left in the hybrid system. With similar isothermal curings, the **PMI-B7** film shows that >98% of chromophore **B7** is retained quantified by the λ_{max} of the charge-transfer band from UV−vis−NIR absorption spectrum. This result is attributed to the efficient molecular engineering of reducing diene reactivity of highly polarizable phenyltetraenic chromophores toward maleimido dienophiles by incorpotating methoxyl group in the middle of the conjugation bridge.[20] While thin layer chromatography (TLC) indicates that the majority of chromophore **B7** was attached into the polymer backbone *via* DA cycloaddition, the solvent resistance of the cured film is lower in common organic solvents, such as acetone, than the cured film of **PMI-A7**. The difference in solvent resistance between two classes of cured films is suspected from a small amount of cross-linking in **PMI-A7**, evidenced with 10% drop-off in the intensity of its absorption spectrum.

Another interesting phenomenon worth pointing out is that after the isothermal curing, **PMI-B7** shows an apparent blue-shift (8 nm) at the λ_{max} of the intramolecular charge-transfer band at the UV−vis−NIR absorption spectrum (Table 1) as compared to the noncured ones, which is attributed to the resulting less polarizable environment for phenyltetraenic chromophores from the Diels−Alder cycloaddition.[28] Also, the cured films of **PMI-B7** show obviously narrower full-width at half-max (fwhm) compared to the noncured ones, which indicates more homogeneous thin films of **PMI-B7** after the isothermal curing. On the other hand, **PMI/AJL28** shows an apparent red shift of 11 nm in the maximum absorption peak over the isothermal curing, which is believed due to the phase separation resulting from the decomposition of **AJL28** by pendant maleimido groups in **PMI**. As for **PMI-A7**, the changes of both the charge-transfer absorption peak and full-width at half-max (fwhm) are very slight. As the forementioned discussion, we believe that it is the combined contribution from both the less polarizable environment from the Diels−Alder cycloaddition and slight phase-separation resulted from minor chromophore decomposition during the lattice hardening.

In addition, from the UV−vis−NIR absorption analysis, the distinct local charge-transfer absorption peak of anthracene around 350−410 nm shows an evident decrease after isothermal heating at 130 °C, indicating the lattice hardening through Diels−Alder cycloaddition between anthracene and maleimide. In order to further study the *in situ* lattice hardening *via* Diels−Alder reaction, FT-IR spectra study was performed. In Figure 4, the IR spectra of **PMI-A7** before and after curing at 130 °C for 30 min are shown. It is clear that two typical anthracene bands at 1272 and 1017 cm^{-1} experienced a significant drop within the isothermal curing. Furthermore, the significantly lowered peak intensity at 847 cm^{-1}, which corresponds to the C−H out of plane bending vibration of isolated hydrogen atoms in anthracene moieties, indicates the consumption of anthracene moieties. All these results suggest that Diels−Alder reaction went smoothly in the thermal curing of the solid films.

The differential scanning calorimetry (DSC) analysis shows that copolymer **PMI** possesses a clear glass transition temperature (T_g) of 125 °C, as well as an apparent melting point (mp) of 175 °C for compound **A7**. After being isothermally cured at 135 °C, the resulting **PMI-A7** clearly showed a high T_g at 152 °C, which can be attributed to the lattice-hardening *via* the *in situ* side-chain generation and small amount of cross-linking. The enhanced T_g derived from minor cross-linking, in turn, increases temporal stability for the poled films. Compared to our previous highly fluorinated dendritic chromophore-containing, *in situ* generated side-chain polymer,[18] this nondendritic side-chain does not show the plasticizer effect even at the high chromophore number density up to 2.55×10^{20} cm^{-3}. Furthermore, shear-modulation force microscopy (SM-FM),[29,30] a new nanoscale methodology capable of providing direct insight into structural relaxations of NLO materials, was employed to study the thermal behavior in these side-chain polymers. The preliminary results show the cured films of **PMI-A7** possess a clear thermal transition temperature at 156 °C, which is in good

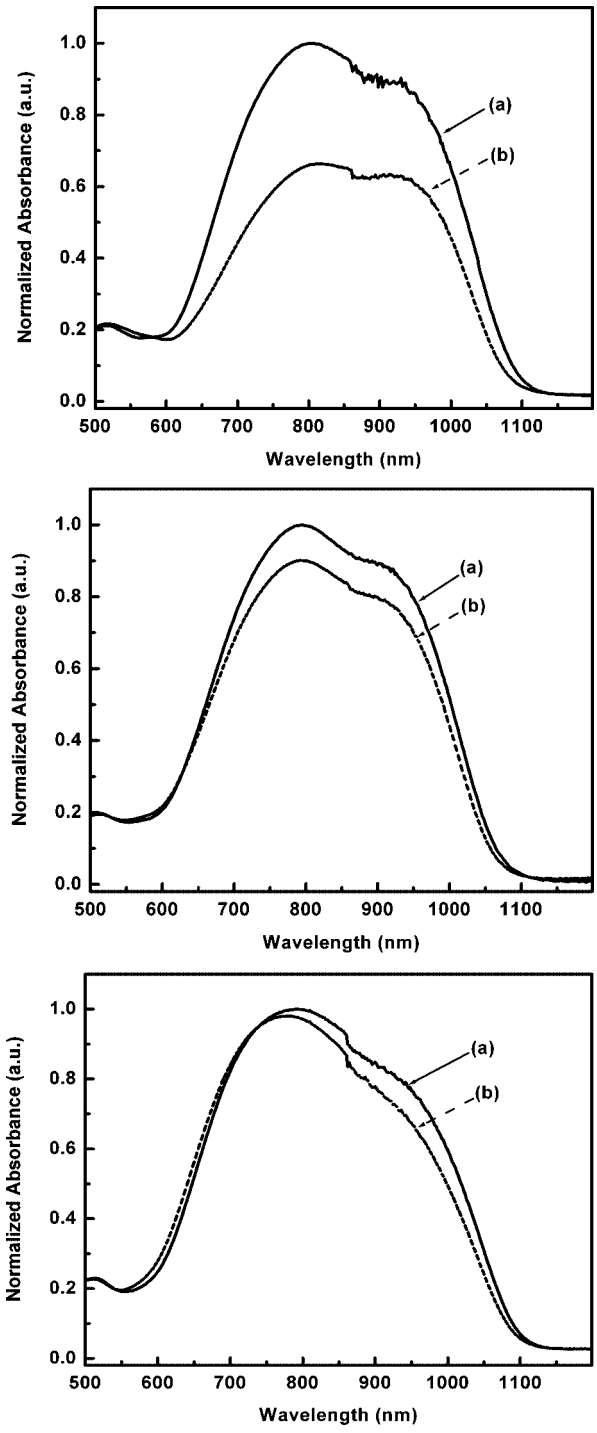

Figure 3. UV−vis−NIR absorption spectra of thin films of **PMI/AJL28**, **PMI-A7**, and **PMI-B7** upon thermal curing at 130 °C for 30 min. The thickness of the films was controlled to be around 0.3 μm. Note that these spectra of thermally cured samples (b) are normalized to those of noncured samples (a).

agreement with the T_g measured by DSC. Comprehensive study for this material system by shear-modulation force microscopy (SM-FM) is actively undergoing and will be reported in due course.

Poling and EO Properties of PMI-A7 and PMI-B7. To study the influence of *in situ* attachment chemistry on poling and E-O properties of **PMI-A7**, and **PMI-B7**, 9 wt % solutions of **PMI-A7**, and **PMI-B7** in 1,1,2-trichloroethane were formulated, filtered through a 0.2-μm PTFE syringe filter, and spin-coated onto ITO substrates respectively. The loading ratio was selected to keep equal equivalent of anthryl and maleimido groups in the materials. After baking overnight at 50 °C under vacuum to remove the residual solvent completely, a thin layer of gold was sputtered onto the films as the top electrode for contact poling. Both poling fields and currents were monitored to optimize the entire process. After cooling to room temperature and removing the poling field, r_{33} values of the poled/cured films were measured using the Teng-Man simple reflection technique at the wavelength of 1.31 μm.[31] The poling conditions and measured r_{33} values of these polymers are tabulated in Table 2. Both poled films of **PMI-A7** and **PMI-B7** show very large r_{33} values of 263 and 287 pm/V respectively, which represent almost 2.5 times over the previous *in situ* generated NLO side-chain polymers with a maximum r_{33} value of 110 pm/V. More importantly, due to the minor amount (10%) of reaction between chromophore **A7** and pendant maleimide groups in polymer (**PMI**), **PMI-A7** has better dielectric strength for poling. As a result, **PMI-A7** polymers can achieve excellent poling efficiency in high poling fields between 100 and 125 V/μm.

A good linear dependence of the r_{33} values versus the poling voltages has been observed, indicating that the *in situ* generated side-chain polymer with a minor amount of cross-linking, is very beneficial to consistent poling behaviors of the material. (Figure 5) Moreover, the poled **PMI-A7** polymers exhibited very promising long-term alignment stability. Over 87% of the original E-O activity could be retained at 85 °C for 550 h, which is a significant improvement over the previous binary systems. Considering good solvent resistance of the poled films, such an excellent temporal stability is attributed to both the effective postfunctionalization of chromophore *via* the DA "click chemistry" and the enhanced polymer rigidity by the minor degree of cross-linking side reactions. This exceptional result demonstrated an effective route to make NLO polymers with combined large E-O activities, excellent temporal stability, and good

Table 1. UV−Vis−NIR Absorption Characteristics of E-O Polymers

	λ_{max} [a]	Γ_s [b]	λ_1 [c]	λ_2 [c]
PMI/AJL28 (noncured)	803	357	666	1023
PMI/AJL28 (cured)	814	355	670	1025
PMI-A7 (noncured)	794	341	661	1002
PMI-A7 (cured)	792	342	656	998
PMI-B7 (noncured)	790	372	647	1019
PMI-B7 (cured)	782	362	639	1001

[a] λ_{max}, the wavelength of maximum absorption (nm). [b] Γ_s, the full-width at half-max or fwhm (nm). [c] λ_1, λ_2, the wavelength of fwhm at blue and red region.

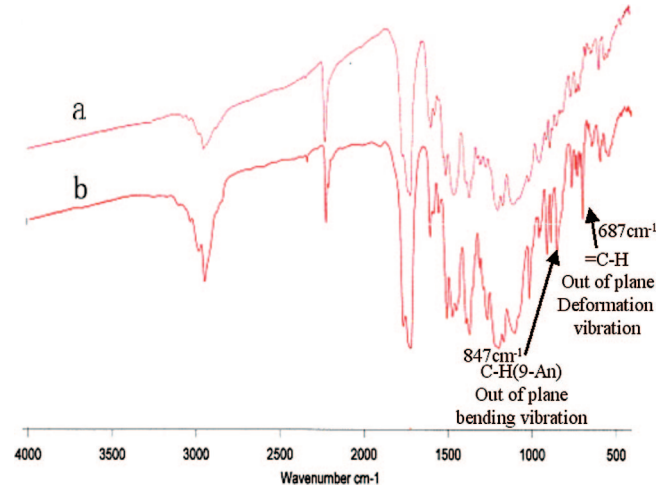

Figure 4. Transmission spectra of (a) **PMI-A7** cured; (b) **PMI-A7** noncured.

Table 2. Summary of Physical Properties of PMI-A7 and PMI-B7, along with Related Parameters

EO polymers[a]	T_g of active dye[b] (°C)	N of dye[c] ($\times 10^{20}$ cm^{-3})	T_{pol}[d] (°C)	poling field (V μm^{-1})	r_{33} at 1.31 μm[e] (pm V^{-1})	normalized r_{33} at 85 °C[f] (%)
PMI-A7	175 (mp)	2.55	135	125	263	87
PMI-B7	97	2.50	116	80	287	61

[a] The weight fractions have been respectively adjusted such that their anthracenyl groups are equivalent to 10 mol % maleimido groups on the polymer. [b] Analytic results of differential scanning calorimetry (DSC) at a heating rate of 10 °C min^{-1} on thermo-equilibrated samples under inert nitrogen for **A7** and **B7**: T_g, glass transition temperatures; mp, melting point. [c] N: the number density of loaded chromophores. $N = N'w\rho/M_w$, where N' is Avogadro's number, M_w is the molecular weight of the chromophore, and ρ is the density of material (with the assumption of $\rho = 1$). [d] T_{pol}: the optimum poling temperature for the poling field. [e] Initial E-O coefficients, r_{33}, measured by a simple reflection technique at 1.31 μm. [f] The percentage of r_{33} values remaining after isothermal heating at 85 °C for 550 h under nitrogen.

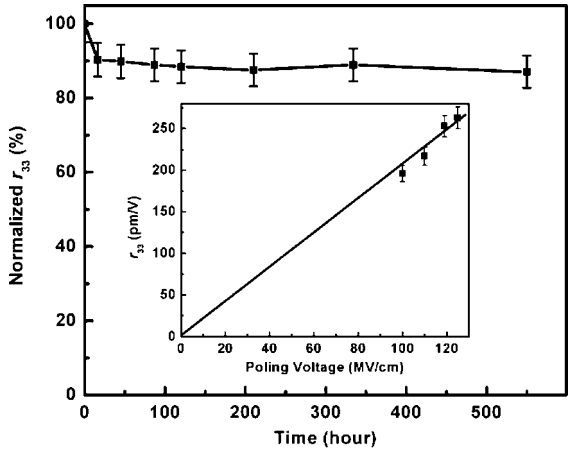

Figure 5. Temporal stability of the poled film **PMI-A7**, which retained about 87% of its original value measured at 1310 nm over 550 h. Inset: r_{33} values measured at a wavelength of 1310 nm as a function of poling fields.

processibility, which are very critical for practical E-O device applications.

Conclusion

Through rational material design, two prototypes of highly efficient and stable NLO side-chain polymers have been systematically exploited to extend the potential for practical device applications. By using a simple and mild DA reaction, highly nonlinear but chemically sensitive phenyltetraenic NLO chromophores could be incorporated into side-chain polymers (**PMI-A7** and **PMI-B7**) to achieve combined good processibility, large E-O coefficients (r_{33}, of up to 287 pm/V at 1.31 μm wavelength), and excellent temporal stability.

Experimental Section

Materials. All reactions were carried out under an inert nitrogen atmosphere unless otherwise specified. Solvents such as tetrahydrofuran (THF) and toluene were treated and distilled prior to use according to common purification procedures. All chemicals from Aldrich were used as received unless otherwise specified. ^{1}H NMR and ^{13}C NMR spectra were taken on a Bruker AV-301 spectrometer (300 MHz) and AV-500 spectrometer (500 MHz) respectively. UV−vis−NIR spectra were obtained on a Perkin-Elmer Lambda-9 spectrophotometer while ESI−MS spectra were recorded on a Bruker Daltonics Esquire ion trap mass spectrometer. Compounds **A1**, **B1**, **AJL28**, and **AJL39** were obtained as solids according to the literature procedures with a minor modification.[20] Compounds **2**, **A5**, and **B5**, were prepared according to procedures found in the literature.[19c,26] Compound **8** was directly used from Aldrich without further purification.

Preparation of Compound A4. To a solution of **A1** (300 mg, 0.66 mmol) in 5 mL of THF was added 2 mL of hydrochloric acid (2 M). The reaction mixture was allowed to stir at room temperature for 0.5 h. Subsequent addition of a few drops of saturated $NaHCO_3$ solution quenched the reaction, and THF was removed under reduced pressure by rotaevaporator. The residual was dissolved in methylenechloride and the organic layer was separated and dried by Na_2SO_4. After removing methylenechloride, the product was obtained as a reddish solid (220 mg, quantitative yield), which was directly used for the next step without further purification. ^{1}H NMR (300 MHz, $CDCl_3$, TMS, ppm): δ 10.23 (d, $J = 8.10$ Hz, 0.33H, *cis*), 10.07 (d, $J = 8.40$ Hz, 0.67H, *trans*),7.34 (d, $J = 8.40$ Hz, 2H), 7.19 (s, 0.33H), 6.75−6.66 (br, 4H), 6.20 (s, 0.67H), 5.93 (d, $J = 8.40$ Hz, 0.67H, *trans*), 5.74 (d, $J = 8.10$ Hz, 0.33H, *cis*), 3.84 (t, $J = 5.85$ Hz, 2H), 3.55−3.44 (m, 4H), 2.69 (s, 2H), 2.37 (s, 2H), 1.21 (t, $J = 7.03$ Hz, 3H), 1.07 (s, 6H). ESI−MS (M^+): calcd, 339.2; found, 339.4.

Preparation of Compound B4. In manner similar to that described above, **B4** was synthesized from **B1** as a reddish solid (quantitative yield). ^{1}H NMR (300 MHz, $CDCl_3$, TMS, ppm): δ 10.11 (d, $J = 8.40$ Hz, 1H), 7.42 (d, $J = 9.00$ Hz, 2H), 7.21 (d, $J = 16.20$ Hz, 1H), 6.76 (d, $J = 9.00$ Hz, 2H), 6.74 (d, $J = 16.50$ Hz, 1H), 6.34 (d, $J = 8.40$ Hz, 1H), 3.84 (t, $J = 5.80$ Hz, 2H), 3.66 (s, 3H), 3.53 (t, $J = 5.80$ Hz, 2H), 3.47 (q, $J = 5.25$ Hz, 2H), 2.75 (s, 2H), 2.37 (s, 2H), 1.21 (t, $J = 7.00$ Hz, 3H), 1.08 (s, 6H). ^{13}C NMR (500 MHz, $CDCl_3$, TMS, ppm): δ 191.43, 151.63, 149.66, 148.65, 132.94, 132.78, 128.70, 125.34, 121.76, 119.73, 112.38, 61.20, 60.80, 52.49, 39.21, 38.94, 30.85, 28.41, 12.16. ESI−MS (M^+): calcd, 369.2; found, 369.5.

Preparation of Compound A6. A solution of compound **A4** (0.20 g, 0.588 mmol), compound **A5** (0.27 g, 0.88 mmol), and 4-(dimethylamino)pyridinium 4-toluenesulfonate (DPTS, 0.02 g, 0.0206 mmol) in THF (15 mL) was stirred overnight after slowly adding dicyclohexylcarbodiimide (DCC, 0.182 g, 0.88 mmol). After carefully removing the resultant urea *via* filtration, all the solvent was evaporated in vacuo. The crude product was purified by column chromatography using ethyl acetate and hexane (1:3, v/v) as the eluent to afford compound 4 as a red solid (0.325 g, 0.52 mmol, yield: 87%). ^{1}H NMR (300 MHz, $CDCl_3$, TMS, ppm): δ 10.11 (d, $J = 8.10$ Hz, 0.3H, *cis*), 9.93 (d, $J = 8.40$ Hz, 0.7H, *trans*),8.36 (s, 1H), 8.22 (d, $J = 9.00$ Hz, 2H), 7.90 (d, $J = 8.10$ Hz, 2H), 7.47 (t, $J = 7.65$, 2H), 7.37 (d, $J = 7.50$ Hz, 2H), 7.19 (d, $J = 9.00$ Hz, 2H), 7.06 (s, 0.3H), 6.62 (d, $J = 9.60$ Hz, 2H), 6.49 (d, $J = 8.70$ Hz, 2H), 6.14 (s, 0.7H), 6.06 (s, 2H), 5.82 (d, $J = 8.40$ Hz, 0.7H, *trans*), 5.62 (d, $J = 8.10$ Hz, 0.3H, *cis*), 4.03 (t, $J = 7.20$ Hz, 2H), 3.29−3.18 (m, 4H), 2.55 (s, 2H), 2.53−2.49 (m, 4H), 2.22 (s, 2H), 1.00 (t, $J = 6.90$ Hz, 3H), 0.94 (s, 6H). ^{13}C NMR (500 MHz, $CDCl_3$, TMS, ppm): δ 190.70, 189.74, 172.46, 172.19, 157.13, 146.75, 132.33, 131.46, 131.15, 129.40, 129.24, 128.58, 128.09, 126.81, 126.29, 126.14, 125.25, 124.03, 111.95, 61.84, 59.26, 39.59, 39.29, 39.00, 31.28, 31.18, 29.23, 29.20, 28.51, 28.38, 12.35. ESI−MS (M^+): calcd, 629.3; found, 629.9.

Preparation of Compound B6. In a manner similar to that described above, **B6** was synthesized from **B4** and **B5** as a reddish solid (yield: 83%). ^{1}H NMR (500 MHz, $CDCl_3$, TMS, ppm): δ 10.14 (d, $J = 8.50$ Hz, 1H), 8.38 (s, 1H), 8.26 (d, $J = 8.50$ Hz, 2H), 8.03 (d, $J = 8.50$ Hz, 2H), 7.56 (t, $J = 8.50$, 2H), 7.50 (t, $J = 7.50$, 2H), 7.44 (d, $J = 8.50$ Hz, 2H), 7.29 (d, $J = 16.50$ Hz, 1H), 6.74 (d, $J = 16.50$ Hz, 1H), 6.71 (d, $J = 9.00$ Hz, 2H), 6.39 (d, $J = 9.00$ Hz, 1H), 4.30 (t, $J = 6.50$ Hz, 2H), 3.98 (t, $J = 8.50$ Hz, 2H), 3.68 (s, 3H), 3.51 (t, $J = 6.50$ Hz, 2H), 3.39 (q, $J = 7.00$ Hz, 2H), 2.81 (t, $J = 8.00$ Hz, 2H), 2.76 (s, 2H), 2.42 (s, 2H), 1.18 (t, $J = 7.00$ Hz, 3H), 1.11 (s, 6H). ^{13}C NMR (500 MHz, $CDCl_3$,

TMS, ppm): δ 191.22, 173.01, 151.33, 149.61, 147.94, 132.72, 132.65, 132.20 131.60, 129.40, 128.66, 126.52, 126.04, 125.26, 124.99, 123.88, 121.74, 119.69, 111.89, 61.84, 61.08, 48.53, 45.19, 41.04, 39.09, 38.83, 35.29, 31.92, 30.73, 28.85, 28.32, 25.21, 23.26, 22.89, 14.15, 12.28. ESI−MS (M^+): calcd, 601.3; found, 601.5.

Preparation of Compound A7. Compound **A6** (0.100 g, 0.16 mmol) and compound **2** (0.057 g, 0.18 mmol) were mixed together with anhydrous ethanol (1.5 mL). The reaction mixture was allowed to stir at 65 °C for about 30 min and monitored by thin layer chromatography (TLC). Solvent was removed in vacuo and the residual mixture was purified by flash chromatography (silica gel; ethyl acetate/hexane = 1:4 to 1:1, v/v) to give compound **A7** as a deep green solid (0.119 g, yield: 80%). ^{1}H NMR (300 MHz, $CDCl_3$, TMS, ppm): δ 8.51 (s, 1H), 8.35 (d, J = 8.70 Hz, 2H), 8.04 (overlap, 3H), 7.62−7.47 (m, 10H), 7.36 (d, J = 9.00 Hz, 2H), 6.89 (d, J = 14.70 Hz, 1H), 6.79 (d, J = 14.70 Hz, 1H), 6.65 (d, J = 9.00 Hz, 2H), 6.37−6.6.29 (overlap, 3H), 6.20 (s, 2H), 4.15 (t, J = 6.30 Hz, 2H), 3.44−3.37 (m, 4H), 2.65−2.62 (m, 4H), 2.41 (s, 2H), 2.39−2.20 (m, 2H), 1.15 (t, J = 7.05 Hz, 3H), 1.03 (s, 3H), 0.97 (s, 3H). ^{13}C NMR (500 MHz, $CDCl_3$, TMS, ppm): δ 176.03, 172.49, 172.24, 162.19, 159.15, 152.32, 146.77, 145.54, 136.35, 131.53, 131.46, 131.39, 131.21, 130.42, 130.22, 129.74, 129.69, 129.47, 129.31, 128.85, 126.89, 126.59, 126.16, 125.32, 124.08, 123.46, 121.19, 115.68, 112.17, 112.07, 111.76, 111.24, 111.19, 95.98, 95.73, 61.72, 59.36, 57.03, 48.65, 47.26, 45.56, 39.98, 39.71, 32,09, 31.76, 29.27, 29.23, 28.74, 28.43, 28.30, 28.24, 12.41. ESI−MS (M^+): calcd, 926.4; found, 926.5.

Preparation of Compound B7. In a manner similar to that described above, **B7** was synthesized from **B6** and compound **2** as a deep green solid (yield: 86%). ^{1}H NMR (500 MHz, $CDCl_3$, TMS, ppm): δ 8.41 (s, 1H), 8.25 (d, J = 8.70 Hz, 2H), 8.04 (overlap, 3H), 7.60−7.48 (m, 10H), 7.45 (d, J = 9.00 Hz, 2H), 7.29 (d, J = 16.00 Hz, 2H), 6.89 (d, J = 16.00 Hz, 1H), 6.78 (d, J = 12.50 Hz, 1H), 6.71 (d, J = 9.00 Hz, 2H), 6.50 (d, J = 14.5 Hz, 1H), 4.30 (t, J = 6.00 Hz, 2H), 3.98 (t, J = 8.00 Hz, 2H), 3.69 (s, 3H), 3.55 (t, J = 6.00 Hz, 2H), 3.41 (q, J = 7.00 Hz, 2H), 2.82 (t, J = 8.00 Hz, 2H), 2.46 (s, 2H), 2.40−2.27 (m, 2H), 1.20 (t, J = 7.00 Hz, 3H), 1.05 (s, 3H), 1.00 (s, 3H). ^{13}C NMR (500 MHz, $CDCl_3$, TMS, ppm): δ 175.90, 173.13, 162.45, 152.05, 151.56, 148.97, 146.85, 138.65, 136.28, 132.27, 131.73, 131.45, 130.26, 129.79, 129.76, 129.63, 129.53, 126.91, 126.65, 126.17, 125.20, 125.12, 123.98, 123.75, 119.77, 116.84, 112.11, 111.88, 111.59, 111.09, 61.83, 61.79, 57.59, 48.64, 45.43, 40.15, 39.36, 35.39, 31.24, 28.65, 28.09, 23.36, 12.40. ESI−MS (M^+): calcd, 898.3; found, 898.5.

Preparation of PMI10 via Postfunctionalization. To a mixture of poly(4-vinylphenol-*co*-methyl methacrylate) (hydroxyphenyl groups = 6.0 mmol) and 4-maleimidobenzoic acid chloride (1.2 mmol) in 20 mL of THF in an ice bath, diisopropylethylamine (1.15 mmol) was added slowly as an acid acceptor followed by stirring for another 1 h. The mixture was then warmed to room temperature and stirred for 0.5 h. Subsequently, the reaction solution was cooled down to 0 °C again. Acetyl chloride (10 mmol) and diisopropylethylamine (7.5 mmol) were added slowly and the reaction solution was stirred overnight. Afterward, the resulting polymer was poured into a large excess of methanol and separated by filtration. The pure polymer was obtained by another precipitation in methanol (degree of phenol termination: 100% by IR). ^{1}H NMR (300 MHz, $CDCl_3$, TMS, ppm): δ 8.43 (d, J = 8.40 Hz, 2H), 7.71 (d, J = 8.70 Hz, 2H), 7.25−6.74 (m, 22H), 3.60 (br, 14H), 3.13 (br, 5H), 2.37 (s, 6H), 2.01−1.43 (br, 10H), 0.87 (s, 14H).

Acknowledgment. Financial support for this work from the National Science Foundation (NSF-STC Program under Agreement Number DMR-0120967), Intel Corporation, the Office of Naval Research (ONR), the Air Force Office of Scientific Research (AFOSR), UIF graduate fellowship through the Center for Nanotechnology at the University of Washington, and Boeing-Johnson Foundation are acknowledged.

References and Notes

(1) (a) Shi, Y.; Zhang, C.; Zhang, H.; Bechtel, J. H.; Dalton, L. R.; Robinson, B. H.; Steier, W. H. *Science* **2000**, *288*, 119–122. (b) Lee, M.; Katz, H. E.; Erben, C. D.; Gill, M.; Gopalan, P.; Heber, J. D.; McGee, D. J. *Science* **2002**, *298*, 1401–1403. (c) Enami, Y.; DeRose, C. T.; Mathine, D.; Loychik, C.; Greenlee, C.; Norwood, R. A.; Kim, T. D.; Luo, J.; Tian, Y.; Jen, A. K.-Y.; Peyghambarian, N. *Nature Photonics* **2007**, *1*, 183–185. (d) Facchetti, A.; Annoni, E.; Beverina, L.; Morone, M.; Zhu, P.; Marks, T.; Pagani, G. *Nat. Mater.* **2004**, *3*, 910–917.

(2) (a) Hochberg, M.; Baehr-Jones, T.; Wang, G.; Shearn, M.; Harvard, K.; Luo, J.; Chen, B.; Shi, Z.; Lawson, R.; Sullivan, P.; Jen, A. K.-Y.; Dalton, L.; Scherer, A. *Nat. Mater.* **2006**, *5*, 703–709. (b) Saadeh, H.; Wang, L.; Yu, L. *J. Am. Chem. Soc.* **2000**, *122*, 546–547. (c) Kajzar, F.; Lee, K.-S.; Jen, A. K.-Y. *Adv. Polym. Sci.* **2003**, *161*, 1–85. (d) Kim, T.-D.; Kang, J.-W.; Luo, J.; Jang, S.-H.; Ka, J.-W.; Tucker, N.; Benedict, J.; Dalton, L.; Gray, T.; Overney, R.; Park, D.-H.; Herman, W.; Jen, A. K.-Y. *J. Am. Chem. Soc.* **2007**, *129*, 488–489. (e) Sullivan, P.; Rommel, H.; Liao, Y.; Olbricht, B.; Akelaitis, A.; Firestone, K.; Kang, J.-W.; Luo, J.; Davies, J.; Choi, D.-H.; Eichinger, B.; Reid, P.; Chen, A.; Jen, A. K.-Y.; Robinson, B.; Dalton, L. *J. Am. Chem. Soc.* **2007**, *129*, 7523–7530. (f) Block, B. A.; Younkin, T. R.; Davids, P. S.; Reshotko, M. R.; Chang, P.; Polishak, B. M.; Huang, S.; Luo, J. O.; Jen, A. K.-Y. *Opt. Express* **2008**, *16*, 18326.

(3) (a) Dalton, L. R.; Steier, W. H.; Robinson, B. H.; Zhang, C.; Ren, A.; Garner, S.; Chen, A.; Londergan, T.; Irwin, L.; Carlson, B.; Fifield, L.; Phelan, G.; Kincaid, C.; Amend, J.; Jen, A. K.-Y. *J. Mater. Chem.* **1999**, *9*, 1905–1920. (b) Prasad, P. N.; Williams, D. J. *Introduction to Nonlinear Optical Effects in Molecules and Polymers*; John Wiley and Sons: New York, 1991. (c) *Advanced Functional Molecules and polymers*; Nalwa, H. S., Ed.; Gordon and Breach Science Publishers: Los Angeles, 2001; Chapter 5, pp 229−260.

(4) Burland, D. M.; Miller, R. D.; Walsh, C. A. *Chem. Rev.* **1994**, *94*, 31–75.

(5) (a) Luo, J.; Liu, S.; Haller, M.; Liu, L.; Ma, H.; Jen, A.K.-Y. *Adv. Mater.* **2002**, *14*, 1763–1768. (b) Saadeh, H.; Yu, D.; Wang, L. M.; Yu, L. P. *J. Mater. Chem.* **1999**, *9*, 1865–1873. (c) Liao, Y.; Anderson, C. A.; Sullivan, P. A.; Akelaitis, A. J. P.; Robinson, B. H.; Dalton, L. R. *Chem. Mater.* **2006**, *18*, 1062–1067. (d) Miller, R. D.; Burland, D. M.; Jurich, M.; Lee, V. Y.; Moylan, C. R.; Thackara, J. I.; Twieg, R. J.; Verbiest, T.; Volksen, W. *Macromolecules* **1995**, *28*, 4970–4974. (e) Song, N.; Men, L.; Gao, J.; Bai, Y.; Yu, G.; Beaudin, A.; Wang, Z.-Y. *Chem. Mater.* **2004**, *16*, 3708–3713.

(6) Chen, T.-A.; Jen, A. K.-Y.; Cai, Y. *J. Am. Chem. Soc.* **1995**, *117*, 7295–7296.

(7) Jen, A. K.-Y.; Liu, Y.-J.; Cai, Y.; Rao, V. P.; Dalton, L. R. J. *Chem. Soc., Chem. Commun.* **1994**, 2711–2712.

(8) Wang, X.; Chen, J.-I.; Marturunkakul, S.; Li, L.; Kumar, J.; Tripathy, S. K. *Chem. Mater.* **1997**, *9*, 45–50.

(9) Luo, J.; Qin, J.; Kang, H.; Ye, C. *Chem. Mater.* **2001**, *13*, 927–931.

(10) Luo, J.; Haller, M.; Li, H.; Tang, H.; Jen, A. K.-Y.; Jakka, K.; Chou, C.; Shu, C. *Macromolecules* **2004**, *37*, 248–250.

(11) Kolb, H. C.; Finn, M. G.; Sharpless, K. B. *Angew. Chem., Int. Ed.* **2001**, *40*, 2004–2021.

(12) (a) Parrish, B.; Breitenkamp, R. B.; Emrick, T. *J. Am. Chem. Soc.* **2005**, *127*, 7404–7410. (b) Stocking, E. M.; Williams, R. M. *Angew. Chem., Int. Ed.* **2003**, *42*, 3078–3115.

(13) (a) Ramachary, D. B.; Barbas, C. F. *Chem.—Eur. J.* **2004**, *10*, 5323–5331. (b) Urien, M.; Erothu, H.; Cloutet, E.; Hiorns, R. C.; Vignau, L.; Cramail, H. *Macromolecules* **2008**, *41*, 7033–7040.

(14) (a) Britcher, L.; Barnes, T. J.; Griesser, H. J.; Prestidge, C. A. *Langmuir* **2008**, *24*, 7625–7627. (b) Zhou, Y.; Wang, S.; Zhang, K.; Jiang, X. *Angew. Chem., Int. Ed.* **2008**, *47*, 7454–7456.

(15) (a) Helms, B.; Mynar, J. L.; Hawker, C. J.; Fréchet, J. M. J. *J. Am. Chem. Soc.* **2004**, *126*, 15020–15021. (b) Tasdelen, M. A.; Van Camp, W.; Goethals, E.; Dubois, P.; Du Prez, F.; Yagci, Y. *Macromolecules* **2008**, *41*, 6035–6040. (c) Killops, K. L.; Campos, L. M.; Hawker, C. J. *J. Am. Chem. Soc.* **2008**, *130*, 5062–5064.

(16) (a) Kim, T.-D.; Luo, J.; Tian, Y.; Ka, J.-W.; Tucker, N.; Haller, M.; Kang, J.-W.; Jen, A. K.-Y. *Macromolecules* **2006**, *39*, 1676–1680. (b) Shi, Z.; Luo, J.; Huang, S.; Zhou, X.-H.; Kim, T.-D.; Cheng, Y.-J.; Polishak, B.; Youkin, T.; Block, B.; Jen, A. K.-Y. *Chem. Mater.* **2008**, *20*, 6372–6377.

(17) (a) Zeng, Q.; Li, Z.; Li, Z.; Ye, C.; Qin, J.; Tang, B.-Z. *Macromolecules* **2007**, *40*, 5634–5637. (b) Li, Z.; Zeng, Q.; Li, Z.; Dong, S.; Zhu, Z.; Li, Q.; Ye, C.; Di, C.; Liu, Y.; Qin, J. *Macromolecules* **2006**, *39*, 8544–8546.

(18) Kang, J.-W.; Kim, T.-D.; Luo, J.; Haller, M.; Jen, A. K.-Y. *Appl. Phys. Lett.* **2005**, *87*, 071109/1–071109/3.

(19) (a) Marder, S. R.; Cheng, L.-T.; Tiemann, B. G.; Friedli, A. C.; Blanchard-Desce, M.; Perry, J. W.; Skindhoj, J. *Science* **1994**, *263*, 511–514. (b) Dalton, L. R. *J. Phys.: Condens. Matter* **2003**, *15*,

R897−R934. (c) Liu, S.; Haller, M.; Ma, H.; Dalton, L.; Jang, S.-H.; Jen, A. K.-Y. *Adv. Mater.* **2003**, *15*, 603–607.
(20) Luo, J.; Huang, S.; Cheng, Y.-J.; Kim, T.-D.; Shi, Z.; Zhou, X.-H.; Jen, A. K.-Y. *Org. Lett.* **2007**, *9*, 4471–4474.
(21) (a) Jen, A.; Luo, J.; Kim, T. D.; Chen, B.; Jang, S. H.; Kang, J. W.; Tucker, N.; Hau, S.; Tian, Y.; Ka, J. W.; Haller, M.; Liao, Y.; Robinson, B.; Dalton, L.; Herman, W. *Proc. SPIE−Int. Soc. Opt. Eng.* **2005**, *5935*, 593506/1–593506/13 (Linear and Nonlinear Optics of Organic Materials). (b) Zhang, C.; Dalton, L. R.; Oh, M.-C.; Zhang, H.; Steier, W. H. *Chem. Mater.* **2001**, *13*, 3043–3050.
(22) For example: (a) Kanis, D. R.; Ratner, M. A.; Marks, T. J. *Chem. Rev* **1994**, *94*, 195–242. (b) Bredas, J. L.; Adant, C.; Tackx, P.; Persoons, A.; Pierce, B. M. *Chem. Rev.* **1994**, *94*, 243–278.
(23) Dalton, L. R.; Harper, A. W.; Ghosn, R.; Steier, W. H.; Ziari, M.; Fetterman, H.; Shi, Y.; Mustacich, R. V.; Jen, A. K.-Y.; Shea, K. J. *Chem. Mater.* **1995**, *7*, 1060–1081.
(24) Meerholz, K.; Nardin, Y.; Bittner, R.; Wortmann, R.; Wurthner, F. *Appl. Phys. Lett.* **1998**, *73*, 4–6.
(25) Palffy-Muhoray, P.; Dunmer, D.; Price, A. *Chem. Phys. Lett.* **1982**, *93*, 572–577.
(26) Kim, T.-D.; Kang, J.-W.; Luo, J.; Chen, B.; Ka, J.-W.; Jang, S.-H.; Tucker, N.; Shi, Z.; Haller, M.; Hau, S.; Jen, A. K.-Y. *Proc. SPIE−Int. Soc. Opt. Eng.* **2005**, *5935*, 593505/1–593505/11.
(27) Kim, T.-D.; Luo, J.; Ka, J.-W.; Hau, S.; Tian, Y.; Shi, Z.; Tucker, N.; Jang, S.-H.; Kang, J.-W.; Jen, A. K.-Y. *Adv. Mater.* **2006**, *18*, 3038–3042.
(28) Shi, Z.; Hau, S.; Luo, J.; Kim, T.-D.; Tucker, N. M.; Ka, J.-W.; Sun, H.; Pyajt, A.; Dalton, L.; Chen, A.; Jen, A. K.-Y. *Adv. Funct. Mater.* **2007**, *17*, 2557–2563.
(29) Gray, T.; Killgore, J.; Luo, J.; Jen, A. K.-Y.; Overney, R. *Nanotechnology* **2007**, *18*, 044009/1–044009/9.
(30) Gray, T.; Kim, T.-D.; Knorr, D. B.Jr.; Luo, J.; Jen, A. K.-Y.; Overney, R. *Nano. Lett* **2008**, *8*, 754–759.
(31) Teng, C. C.; Man, H. T. *Appl. Phys. Lett.* **1990**, *56*, 1734–1736.

MA802612G